SFN 300 No.11-20

2017/12/22

担当　原田遼平

11. Very Low-mass Stars and Brown Dwarfs in Upper Scorpius Using Gaia DR1: Mass Function, Disks, and Kinematics
12. Widespread SiO and CH3OH Emission in Filamentary Infrared-Dark Clouds
13. Protoplanetary Disks in ρ Ophiuchus as Seen From ALMA
14. Probing the origin of UX Ori-type variability in the YSO binary CO Ori with VLTI/GRAVITY
15. New insights in the mid-infrared bubble N49 site: a clue of collision of filamentary molecular clouds
16. ALMA continuum observations of the protoplanetary disk AS 209. Evidence of multiple gaps opened by a single planet
17. The evolution of surface magnetic fields in young solar-type stars II: The early main sequence (250–650 Myr)
18. Twelve Years of Spectroscopic Monitoring in the Galactic Center: The Closest Look at S-stars near the Black Hole
19. The Evolution of Supermassive Population III Stars
20. A likely planet-induced gap in the disk around T Cha

#11

Very Low-mass Stars and Brown Dwarfs in Upper Scorpius Using Gaia DR1: Mass Function, Disks, and Kinematics

Our understanding of the brown dwarf population in star forming regions is dependent on knowing distances and proper motions, and therefore will be improved through the Gaia space mission. In this paper, we select new samples of very low mass objects (VLMOs) in Upper Scorpius using UKIDSS colors and optimised proper motions calculated using Gaia DR1. The scatter in proper motions from VLMOs in Upper Scorpius is now (for the first time) dominated by the kinematic spread of the region itself, not by the positional uncertainties. With age and mass estimates updated using Gaia parallaxes for early type stars in the same region, we determine masses for all VLMOs. Our final most complete sample includes 453 VLMOs of which ~125 are expected to be brown dwarfs. The cleanest sample is comprised of 131 VLMOs, with ~105 brown dwarfs. We also compile a joint sample from the literature which includes 415 VLMOs, out of which 152 are likely brown dwarfs. The disc fraction among low-mass brown dwarfs ($M < 0.05\ M_\odot$) is substantially higher than in more massive objects, indicating that discs around low-mass brown dwarfs survive longer than in low- mass stars overall. The mass function for $0.01 < M < 0.1\ M_\odot$ is consistent with the Kroupa IMF. We investigate the possibility that some 'proper motion outliers' have undergone a dynamical ejection early in their evolution. Our analysis shows that the color-magnitude cuts used when selecting samples introduce strong bias into the population statistics due to varying level of contamination and completeness.

- UKIDSSカラーを用いてUpper ScorpiusでVLMO（very low mass object）の新しいサンプルを選択し、固有運動を最適化した
- ガイア視差を用いて年齢および質量推定値を更新すると、すべてのVLMOの質量が決定
- 453個のVLMOが含まれており、うち～125個は褐色矮星であると予想
- 小質量褐色矮星（M <0.05 M☉）のdisk fractionは、より重いものよりも高く、小質量褐色矮星ディスクは全体的な小質量星より長く生き残る
- 0.01 <M <0.1$M_\odot$の質量関数は、Kroupa IMFと一致

#12

Widespread SiO and CH_3OH Emission in Filamentary Infrared-Dark Clouds

G. Cosentino1, I. Jim´enez-Serra2, J. D. Henshaw3, P. Caselli4, S. Viti1, A. T. Barnes3,4, F. Fontani6, J. C. Tan5 and A. Pon

https://arxiv.org/pdf/1711.09679.pdf

- 赤外線暗黒星雲（IRDC）は、大質量星や星団の生まれる場であり、寒くて高密度の領域
- 3つのIRDC、G028.37 + 00.07、G034に向けて、高密度ガストレーサー（H13CO +およびHN13C）と典型的なショックトレーサー（SiOおよびCH3OH）の輝線マップを取得
  - すべてのクラウドで3つの独立したサブ構造に対応する複数の速度成分を示す
  - 最も明るいサブ構造は、雲の中心速度で移動する周囲のガスをプローブし、赤色と青色にシフトした下位構造は、雲の中心速度に対して1km s^-1シフトした速度をもつ

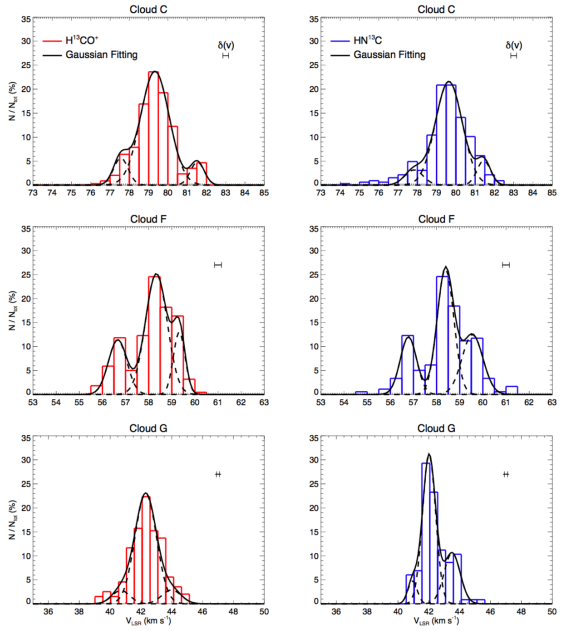

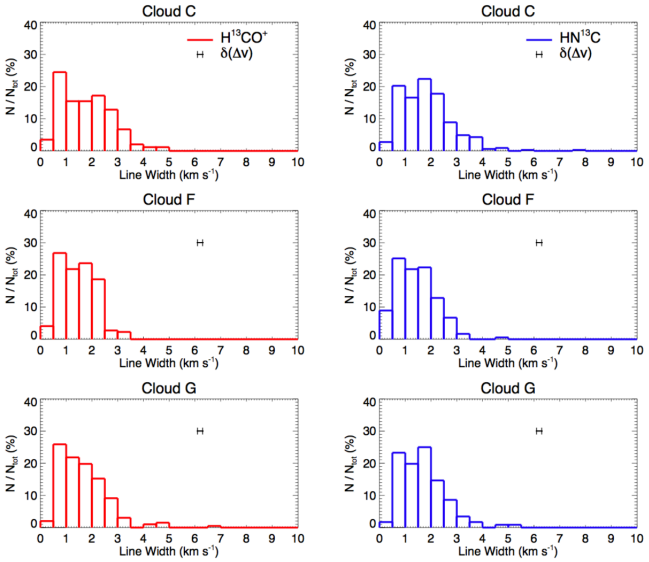

- H13CO +およびHN13Cは同様の線幅を示す(<5km/s)
- 線幅の平均値(1.8km/s)は3つのクラウドで同等

Figure 3

#12

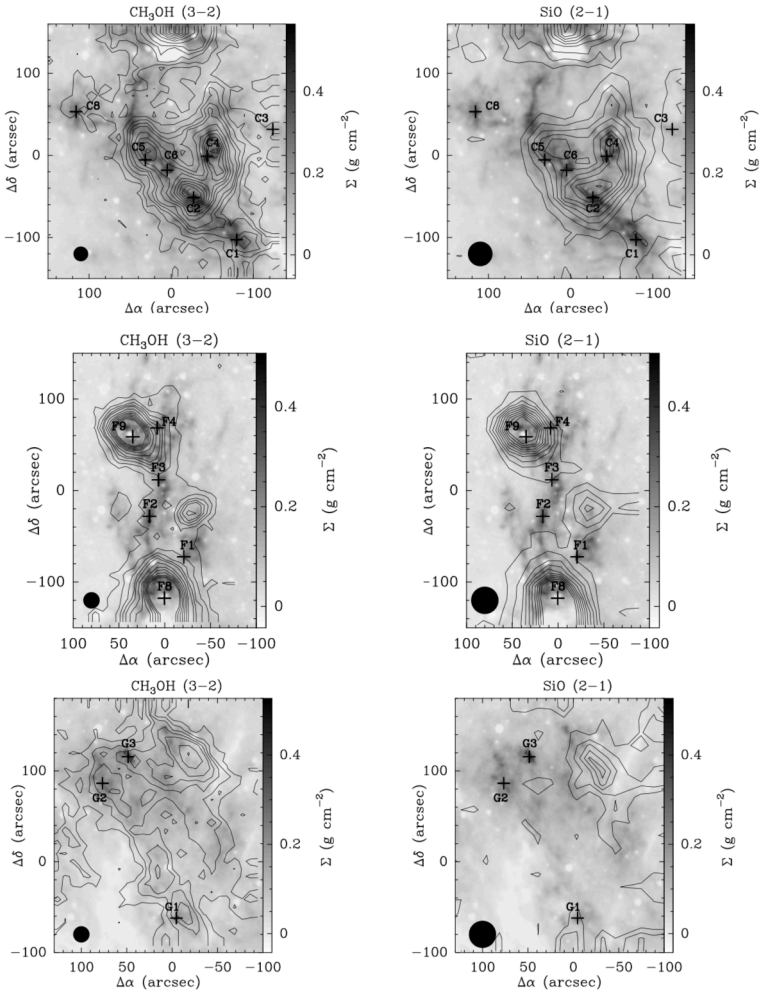

Figure 6

- ショックトレーサーの空間分布は、すべての雲でpcスケールで広がっている
- 雲CおよびFでは、いくつかのコアに見られるが、雲GではSiOおよびCH3OH分布は非常に異なる(コアと相関しない)

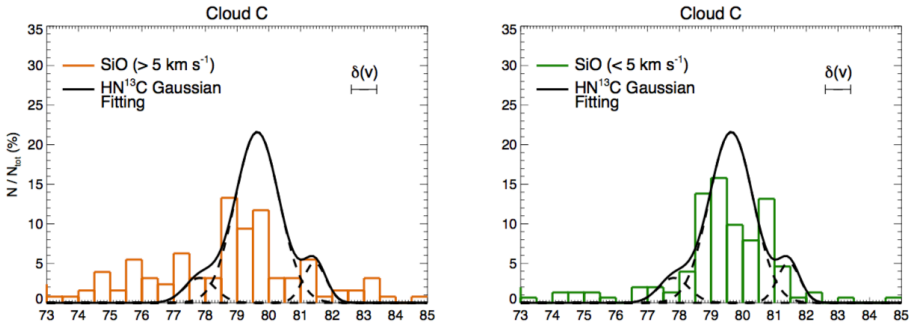

Figure 9

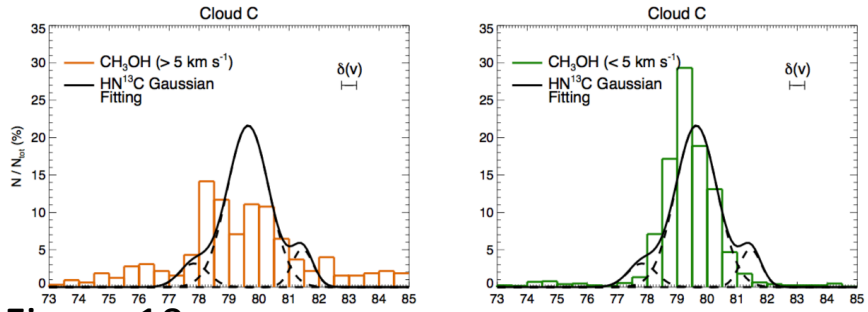

Figure 10

- ショックトレーサは複数の線幅成分を示す：narrow（< 5 km s^-1）は広範囲に存在。broadは(up to 30km s^-1) コアに存在
- SiOおよびCH3OHのbroad成分もnarrow成分も、高密度のサブフィラメント構造に従わない

#12

- 星形成が活発な雲CおよびFについては、広範囲のSiOおよびCH3OHは進行中の星形成活動と関連している可能性が高い
- これらの雲のアウトフローは、衝撃波を受けたガスおよび初期段階のMHD衝撃波の伝播にそれぞれ対応するbroadおよびnarrow成分の両方に関与するであろう。
- 8μm, 24μm sourceがない雲Gの場合、検出された広範囲のSiOおよびCH3OH放射は、大規模な衝撃相互作用に由来する可能性がある
- 雲Gでは、SiOおよびCH3OHの放射は異なる起源
- 特に、SiOは、近くでの以前の大規模な相互作用の化石である可能性がある。
- 雲G中のnarrowなCH3OH放射は、対応するSiO放射よりも広がっており雲の中心速度に近い。
- それは主に静止ガスに付随しており、化学反応脱離機構によって生成される可能性がある

#13

Protoplanetary Disks in ρ Ophiuchus as Seen From ALMA

We present a high angular resolution (~0. 2), high sensitivity (σ ~ 0.2 mJy) survey of the 870 μm continuum emission from the circumstellar material around 49 pre-main sequence stars in the ρ Ophiuchus molecular cloud. Because most millimeter instruments have resided in the northern hemisphere, this represents the largest high-resolution, millimeter- wave survey of the circumstellar disk content of this cloud. Our survey of 49 systems comprises 63 stars; we detect disks associated with 29 single sources, 11 binaries, 3 triple systems and 4 transition disks. We present flux and radius distributions for these systems; in particular, this is the first presentation of a reasonably complete probability distribution of disk radii at millimeter-wavelengths. We also compare the flux distribution of these protoplanetary disks with that of the disk population of the Taurus-Auriga molecular cloud. We find that disks in binaries are both significantly smaller and have much less flux than their counterparts around isolated stars. We compute truncation calculations on our binary sources and find that these disks are too small to have been affected by tidal truncation and posit some explanations for this. Lastly, our survey found 3 candidate gapped disks, one of which is a newly identified transition disk with no signature of a dip in infrared excess in extant observations.

- ρ Ophiuchus 分子雲中の約49個の前主系列星の星周物質からの870 μm連続波放射の高角度分解能（～0.2）、高感度（σ～0.2mJy）の調査
- 29個のシングルソース、11個のバイナリ、3個のトリプルシステム、および4個のトランジションディスクに付随するディスクを検出
- バイナリ内のディスクは、孤立した星のディスクよりもはるかに小さく、フラックスがずっと少ない

#14

Probing the origin of UX Ori-type variability in the YSO binary CO Ori with VLTI/GRAVITY

The primary star in the young stellar object (YSO) binary CO Ori displays UX Ori-type variability: irregular, high amplitude optical and near-infrared photometric fluctuations where flux minima coincide with polarization maxima. This is attributed to changes in local opacity. In CO Ori A, these variations exhibit a 12.4 yr cycle. Here, we investigate the physical origin of the fluctuating opacity and its periodicity using interferometric observations of CO Ori obtained using VLTI/GRAVITY. Continuum K-band circum-primary and circum-secondary emission are marginally spatially resolved for the first time while Brγ emission is detected in the spectrum of the secondary. We estimate a spectral type range for CO Ori B of K2-K5 assuming visual extinction, $A_V = 2$ and a distance of 430 pc. From geometric modelling of the continuum visibilities, the circum-primary emission is consistent with a central point source plus a Gaussian component with a full-width-half-maximum of 2.31±0.04 milliarcseconds (mas), inclined at 30.2±2.2◦ and with a major axis position angle of 40±6◦. This inclination is lower than that reported for the discs of other UX Ori-type stars, providing a first indication that the UX Ori phenomena may arise through fluctuations in circumstellar material exterior to a disc, e.g. in a dusty outflow. An additional wide, symmetric Gaussian component is required to fit the visibilities of CO Ori B, signifying a contribution from scattered light. Finally, closure phases of CO Ori A were used to investigate whether the 12.4 yr periodicity is associated with an undetected third component, as has been previously suggested. We rule out any additional companions contributing more than 3.6

- VLTI / GRAVITYを用いて得られたCO Oriの干渉計観測を用いて、変動する不透明度の物理的起源およびその周期性を調べる。
- 連続波ビジビリティの幾何学的モデリングから、周りの放射は、中心点源と、全幅半値が2.31±0.04ミリ秒（mas）、30.2±2.2◦の傾斜、長軸の位置角は40±6°のガウス成分と一致。
- この傾きは、UX Oriのディスクで報告されている傾きよりも低く、ディスクの外の星周物質の変動によってUX Ori現象が起こる可能性があることを示す。

#15

New insights in the mid-infrared bubble N49 site: a clue of collision of filamentary molecular clouds

L. K. Dewangan1, D. K. Ojha2 and I. Zinchenko

https://arxiv.org/pdf/1711.09679.pdf

- バブルN49と3つのフィラメント（「fl-1」、「fl-2」、「fl-3」）が存在し3つの速度成分が存在。
- Herschelの温度マップではフィラメントは約16-20 Kの温度範囲で見られ、暖かいガス（Td～21-24 K）はN49 HII領域に向かって見られる

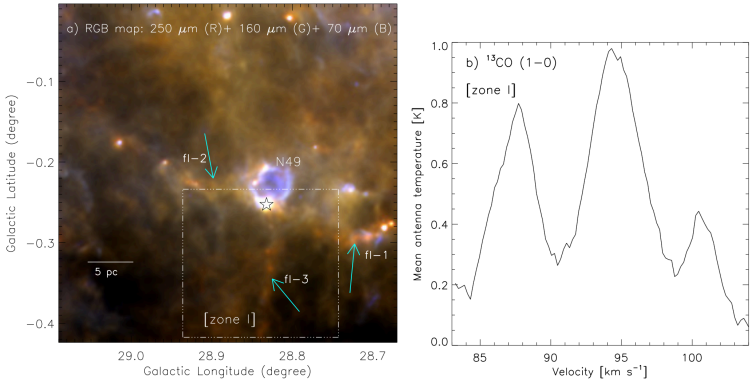

Figure 1

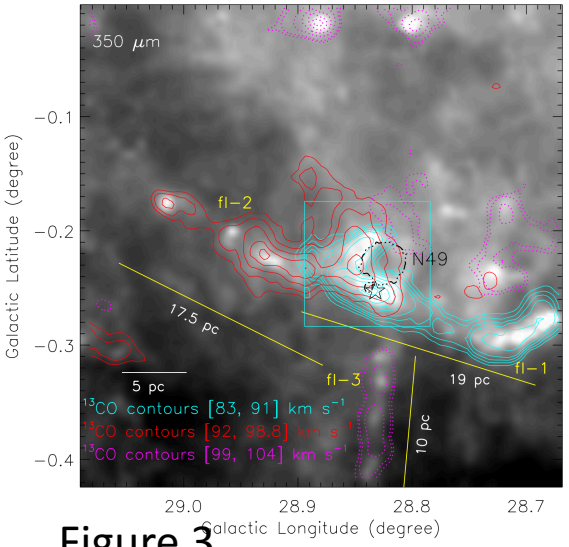

Figure 3

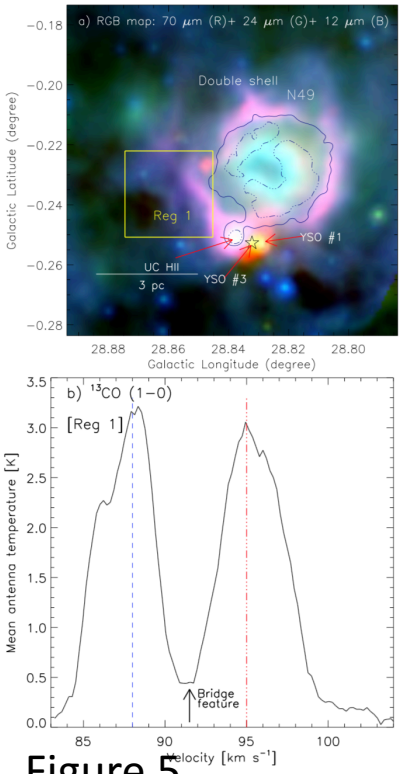

Figure 5

- bubbleは2つのフィラメントに重なって存在
- 2つの速度雲成分がbubbleの方向に存在し、広いブリッジによって相互接続されている。
- 大質量星形成の異なる初期の進化段階（O型星、UCHII領域、および6.7GHz メタノールメーザー）もバブルに存在。

#15

- 2つの雲の速度差（～7 km s^-1）を採用すると、典型的な衝突タイムスケールは約0.7Myr
- クラスIおよびクラスII YSOの平均年齢はそれぞれ~0.44 Myrおよび~1-3 Myr（Evansら、2009）。
- 6.7GHz メタノールメーザーは、大質量星形成の初期段階（<0.1Myr）の存在を示す。
- これらの特徴は、2つのフィラメント状分子雲が約0.7 Myr前にお互いに相互作用したという解釈を支持する
- また、bubbleでの、衝突前に星形成の開始の可能性を却下することはできない

#16 ALMA continuum observations of the protoplanetary disk AS 209. Evidence of multiple gaps opened by a single planet

The paper presents new high angular resolution ALMA 1.3 mm dust continuum observations of the protoplanetary system AS 209 in the Ophiuchus star forming region. The dust continuum emission is characterized by a main central core and two prominent rings at r = 75 au and r = 130 au intervaled by two gaps at at r = 62 au and r = 103 au. The two gaps have different widths and depths, with the inner one being narrower and shallower. We determined the surface density of the millimeter dust grains using the 3D radiative transfer disk code dali. According to our fiducial model the inner gap is partially filled with millimeter grains while the outer gap is largely devoid of dust. The inferred surface density is compared to 3D hydrodynamical simulations (FARGO-3D) of planet-disk interaction. The outer dust gap is consistent with the presence of a giant planet (M_{planet} ~ 0.8 $M_{Staturn}$); the planet is responsible for the gap opening and for the pile-up of dust at the outer edge of the planet orbit. The simulations also show that the same planet can give origin to the inner gap at r = 62 au. The relative position of the two dust gaps is close to the 2:1 resonance and we have investigated the possibility of a second planet inside the inner gap. The resulting surface density (including location, width and depth of the two dust gaps) are in agreement with the observations. The properties of the inner gap pose a strong constraint to the mass of the inner planet (M_{planet} < 0.1 M_J). In both scenarios (single or pair of planets), the hydrodynamical simulations suggest a very low disk viscosity ($\alpha < 10^{-4}$). Given the young age of the system (0.5–1 Myr), this result implies that the formation of giant planets occurs on a timescale of <~1 Myr.

- Ophiuchus領域の原始惑星系AS209の新しい高分解能ALMA1.3mmダスト連続波観測
- ダスト連続体放射は、r = 62auおよびr = 103auの2つのギャップ
- 3D radiative transfer disk code daliを用いてダスト粒子の表面密度を決定した。
- 内部ギャップはミリメートルの粒子で部分的に存在し、外部ギャップにはほとんどダストがない
- 惑星 - ディスク相互作用の3D流体力学シミュレーション（FARGO-3D）と比較すると外側のダストギャップは、巨大な惑星の存在と一致 (M_{planet} ~ 0.8 $M_{Staturn}$)。
- 同じ惑星がr = 62auの内部ギャップの起源となりうることも示している。2つのダストギャップの相対的な位置は2:1の共振に近く、我々は内側のギャップの内側に第2の惑星の可能性を調べ、得られる表面密度（2つのダストギャップの位置、幅および深さを含む）は、観察と一致する

#17 The evolution of surface magnetic fields in young solar-type stars II: The early main sequence (250–650 Myr)

There is a large change in surface rotation rates of sun-like stars on the pre-main sequence and early main sequence. Since these stars have dynamo driven magnetic fields, this implies a strong evolution of their magnetic properties over this time period. The spin-down of these stars is controlled by interactions between stellar winds and magnetic fields, thus magnetic evolution in turn plays an important role in rotational evolution. We present here the second part of a study investigating the evolution of large-scale surface magnetic fields in this critical time period. We observed stars in open clusters and stellar associations with known ages between 120 and 650 Myr, and used spectropolarimetry and Zeeman Doppler Imaging to characterize their large-scale magnetic field strength and geometry. We report 15 stars with magnetic detections here. These stars have masses from 0.8 to 0.95 $M_\odot$, rotation periods from 0.326 to 10.6 days, and we find large-scale magnetic field strengths from 8.5 to 195 G with a wide range of geometries. We find a clear trend towards decreasing magnetic field strength with age, and a power-law decrease in magnetic field strength with Rossby number. There is some tentative evidence for saturation of the large-scale magnetic field strength at Rossby numbers below 0.1, although the saturation point is not yet well defined. Comparing to younger classical T Tauri stars, we support the hypothesis that differences in internal structure produce large differences in observed magnetic fields, however for weak lined T Tauri stars this is less clear.

- 散開星団と120～650 Myrの間の既知の年代を持つ星のアソシエーションを観測し、大規模な磁場強度と形状を特徴付けるために分光偏光法とZeeman Doppler Imagingを使用
- これらの星は、0.8～0.95M⊙の質量を持ち、回転周期は0.326～10.6日であり、広範囲の8.5～195Gの大規模磁場強度がを見つける。
- 年齢とともに磁場強度を減少させる明確な傾向、およびロスビー数による磁場強度のべき乗の減少
- 古典的T Tauri星と比較して、内部構造の違いが観測される磁場の大きな違いを生み出すという仮説を支持

#18

Twelve Years of Spectroscopic Monitoring in the Galactic Center: The Closest Look at S-stars near the Black Hole

We study the young S-stars within a distance of 0.04 pc from the supermassive black hole in the center of our Galaxy. Given how inhospitable the region is for star formation, their presence is more puzzling the younger we estimate their ages. In this study, we analyze the result of 12 years of high-resolution spectroscopy within the central arcsecond of the Galactic Center (GC). By co-adding between 55 and 105 hr of spectra we have obtained high signal-to-noise H- and K-band spectra of eight stars orbiting the central supermassive black hole. Using deep H-band spectra, we show that these stars must be high surface gravity (dwarf) stars. We compare these deep spectra to detailed model atmospheres and stellar evolution models to infer the stellar parameters. Our analysis reveals an effective temperature of 21,000–28,500 K, a rotational velocity of 60–170 km s^{-1}, and a surface gravity of 4.1–4.2. These parameters imply a spectral type of B0–B3V for these stars. The inferred masses lie within 8–14 $M_{\odot}$. We derive an age of $6.6^{+3.4}_{-4.7}$ Myr for the star S2, which is compatible with the age of the clockwise-rotating young stellar disk in the GC. We estimate the ages of all other studied S-stars to be less than 15 Myr, which is compatible with the age of S2 within the uncertainties. The relatively low ages for these S-stars favor a scenario in which the stars formed in a local disk rather than a field binary-disruption scenario that occurred over a longer period of time.

- 銀河の中心にある超大型ブラックホールから0.04 pc離れた若いS型星を研究
- 中央の超大型ブラックホールを周回する8つの星の高いS/NのH-およびK-バンドスペクトルを取得
- 大気および星の進化モデルと比較して、恒星のパラメータを推測すると、有効温度21000-28500 K、回転速度60-170 km / s、表面重力4.1-4.2。
- これらの星はB0-B3Vのスペクトルタイプ。
- 推測される質量は8〜14Mの範囲内にある。
- 星S2について6.6 +3.4 - 4.7 Myrの年齢を導出
- これは、銀河中心の回転する若いstellar diskの年齢に適合

#19

The Evolution of Supermassive Population III Stars

Supermassive primordial stars forming in atomically-cooled halos at z ~ 15 − 20 are currently thought to be the progenitors of the earliest quasars in the Universe. In this picture, the star evolves under accretion rates of 0.1 – 1 $M_\odot$ yr^{-1} until the general relativistic instability triggers its collapse to a black hole at masses of ~ 10^5 $M_\odot$. However, the ability of the accretion flow to sustain such high rates depends crucially on the photospheric properties of the accreting star, because its ionising radiation could reduce or even halt accretion. Here we present new models of supermassive Population III protostars accreting at rates 0.001 – 10 $M_\odot$ yr^{-1}, computed with the GENEVA stellar evolution code including general relativistic corrections to the internal structure. We compute for the first time evolutionary tracks in the mass range M > 105 $M_\odot$. We use the polytropic stability criterion to estimate the mass at which the collapse occurs, which has been shown to give a lower limit of the actual mass at collapse in recent hydrodynamic simulations. We find that at accretion rates higher than 0.01 $M_\odot$ yr^{-1} the stars evolve as red, cool supergiants with surface temperatures below 104 K towards masses > 105 $M_\odot$. Moreover, even with the lower rates 0.001 $M_\odot$ yr^{-1} < dm < 0.01 $M_\odot$ yr^{-1}, the surface temperature is substantially reduced from 105 K to 104 K for M > 600 $M_\odot$. Compared to previous studies, our results extend the range of masses and accretion rates at which the ionising feedback remains weak, reinforcing the case for direct collapse as the origin of the first quasars. We provide numerical tables for the surface properties of our models.

#20

A likely planet-induced gap in the disk around T Cha

Nathanial P. Hendler,1⋆ Paola Pinilla,2 Ilaria Pascucci,1,3 Adriana Pohl,4,5 Gijs Mulders,1,
Thomas Henning,4 Ruobing Dong,2 Cathie Clarke,6 James Owen,7 David Hollenbach

http://arxiv.org/pdf/1711.09933

- T Chaの周りに高度に傾斜した遷移円盤の高分解能（0.11 "x 0.06"）3mm ALMA観測

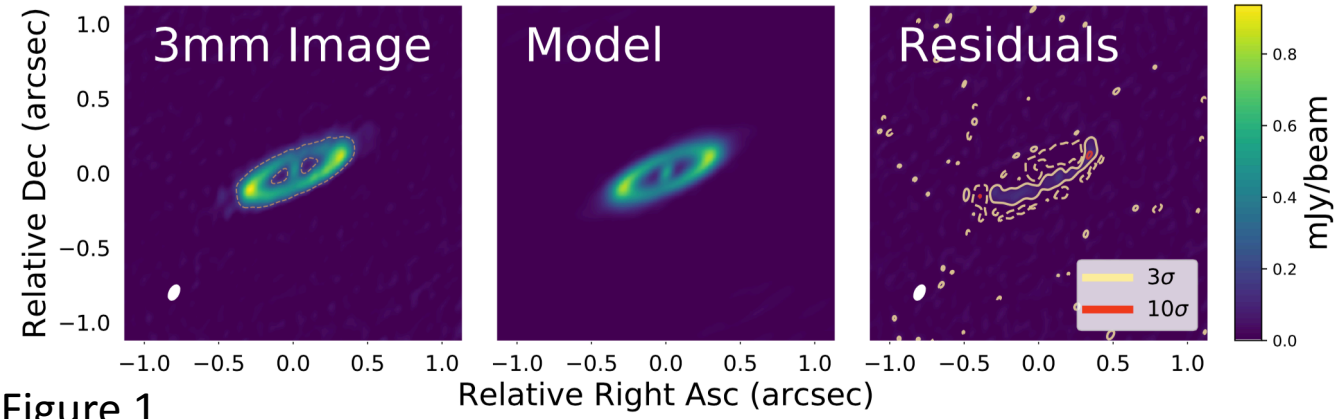

Figure 1

- 複数のダスト構造：内側ディスク、空間的に分解されたダストギャップ、および外側リング
- 3mmビジビリティにsky-brightnessモデルを当てはめると、内側の放射はコンパクトで（<1 au）、ギャップ幅は18～28 auで、外側のリングピークからの放射は～36 au

#20

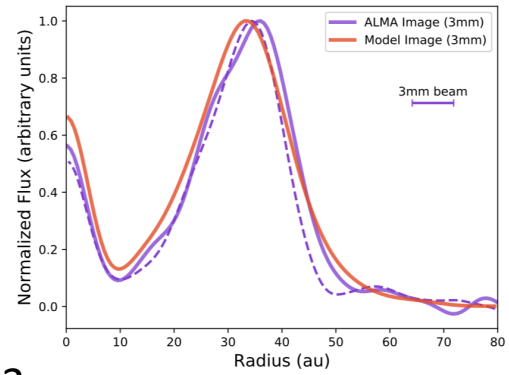

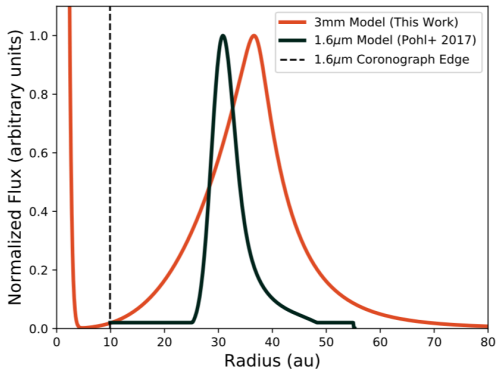

Figure 3

- ALMA画像と、1.6μmVLT / SPHERE画像と比較。
- 外側リングの位置が波長に依存する
- より具体的には、3mmリングのピーク放出は、1.6μmリングの半径方向距離よりも大きく、外側ディスクのミリメートルサイズの粒子は、ミクロンサイズの粒子より中心星から離れて位置することが示唆される
- デッドゾーン、光蒸発、惑星 - ディスク相互作用などのシナリオについて議論
- 粒子の乱流速が低いデッドゾーン内では、粒子成長が効率的であり、小さな粒子が枯渇する。その結果、NIRとmmで同じサイズのキャビティをが期待される
- T Chaの降着率は4 × 10^-9M⊙/year（Schisano et al。2009）。質量増加率とギャップサイズ ≥20auの場合、光蒸発は、T Chaディスクに見られるギャップを開くためのもっともらしいメカニズムであるとは思われない。
- 惑星 - ディスク相互作用モデルからの予想された結果に従って、小さな粒子と大きな粒子との半径方向の分離が観測
- ダストギャップの最も有望な原因は惑星からのものであり、De Juan Ovelar et al. 2013の二次元力学モデルとダスト進化モデルに起因する波長依存の粒子サイズの関係を用いて、単一の惑星シナリオの場合、T Chaのギャップは1.2M_{Jup}の惑星と推定される。